Supplementary Information for:

Timescale for hygroscopic conversion of calcite mineral particles through heterogeneous reaction with nitric acid

Ryan C. Sullivan,[1,†] Meagan J. K. Moore,[1] Markus D. Petters,[2] Sonia M. Kreidenweis,[2] Greg C. Roberts,[3] Kimberly A. Prather[1,3,*]

[1]Department of Chemistry and Biochemistry, University of California, San Diego, La Jolla, CA, 92093

[2]Department of Atmospheric Science, Colorado State University, Fort Collins, CO, 80523

[3]Scripps Institution of Oceanography, University of California, San Diego, La Jolla, CA, 92093

[†]Present address: Department of Atmospheric Science, Colorado State University, Fort Collins, CO, 80523

*Corresponding Author:

Kimberly Prather, Department of Chemistry and Biochemistry and Scripps Institution of Oceanography, University of California, San Diego, 9500 Gilman Drive, La Jolla, CA, 92093-0314, Phone: (858) 822-5312, Fax: (858) 534-7042, e-mail: kprather@ucsd.edu

Supplementary methods

Calibration of HNO_3 permeation tube and HNO_3 flow tube loss

The nitric acid permeation tube's emission rate was empirically measured by bubbling 1.0 sLpm nitrogen gas from the HNO_3 source through the Teflon injector line into 500 mL of $Na_2CO_3/NaHCO_3$ buffer through a glass frit. 5.0 mL aliquots were removed every 30 minutes and the concentration of nitrate was determined by ion chromatography. The measured HNO_3 emission rate was highly linear with time ($R^2=0.99$) and equal to 370.4 ng/min (Fig. S1). The first two aliquots were excluded from the linear fit to eliminate the effect of HNO_3 ad/desorbing from the Teflon injection line and glass frit placed in the water, and to allow the system to reach steady-state. The measured HNO_3 emission rate is 73% of the manufacturer calibrated rate of 507 ng min^{-1} at 30.0 C. This difference is attributed to irreversible loss of HNO_3 in the permeation tube holder and the lines and fittings between the source and end of the injection line.

The $[HNO_3]$ exiting the kinetics flow tube was measured similar to the HNO_3 source calibration, by bubbling the HNO_3 containing gas flow exiting the flow tube into 500 mL of carbonate buffer, and determining the nitrate concentration via ion chromatography in 5.0 mL aliquots every 10 minutes. This produced a linear increase in $[NO_3^-]$ with time ($R^2 > 0.95$), the slope of which corresponded to an observed HNO_3 emission rate of 325 ± 68 ng min^{-1} (n=3). The difference between the HNO_3 source's emission rate and that observed at the end of the flow tube is attributed to irreversible loss to the coated walls of the flow tube, and other surfaces.

CCN activation curve fitting

The lack of a clear minimum plateau from multiply-charged particles in the activation curves of reacted calcite aerosol (Fig. 5) makes it more difficult to accurately fit the curves with a sigmoid curve, defined as:

$$y = \frac{A_1 - A_2}{1 + e^{(x - x_o)/dx}} - A_2 \tag{S1}$$

where y is the measured CCN/CN ratio, A_1 is the minimum value, A_2 is the maximum value, dx is the rate of change, and x_o is the midpoint between A_1 and A_2. The data is normally fit such that A_1 corresponds to the CCN/CN ratio of the multiply charged particles at small supersaturations, and A_2 is set to the scaled maximum CCN/CN ratio of ~1.0. Thus, x_o corresponds to the CCN/CN=0.5 midpoint typically used to define the critical supersaturation (s_c) of the singly-charged particles of interest. The lack of the multiply-charged plateau in the reacted aerosol makes it difficult to empirically constrain A_1 in this fit.

To resolve this issue the contribution of multiply-charged particles in the aerosol exiting the flow tube was directly measured using aerosol size distributions made with a scanning mobility particle sizer (SMPS) composed of a TSI Model 3081 DMA and TSI Model 3010 CPC. Aerosol and sheath flow rates of 0.40 and 4.0 sLpm were used for SMPS scans. The dried and denuded particles were sub-sampled by the SMPS after the flow tube. A typical size distribution is shown in Fig. S2a. The SMPS software's multiple charge correction was not used here. As expected, the dominant mode is centred around 200 nm, which is produced by the original +1 charge 200 nm particles selected by the 1st DMA before the flow tube. The mode to the left are originally +1 200 nm particles that gain a +2 charge in the 2nd DMA, and therefore have a smaller mobility diameter, D_m. The mode on the right are originally +2 charge particles with D_m = 200 nm that only have +1 charge in the 2nd DMA; these represent the physically larger multiply-charged particles in the aerosol measured by the CCNc. The fraction of multiplied charged particles was evaluated from the cumulative % size distribution shown in Fig. S2b. The fraction of particles larger than 250 nm was used to determine the fraction of multiply-charged particles in the aerosol and constrain the value of $A1$ in Eqn. S1. The resulting sigmoid fits are shown along with the data in Fig. 5. The uncertainty in the determination of s_c is typically the product of the uncertainty in the CCNc's SS calibration (3%), and in the particle size selection of the DMA ($\leq$ 5%). The lack of a multiply-charged plateau in the activation curve introduces additional uncertainty in the determination of s_c, though this is constrained by the SMPS measurement. The fraction of multiply-charged particles typically varied by 3% (absolute) between experiments. The value of $A1$ was varied by ±3% (absolute) for fitting several typical activation curves with Eqn. (S1) and produced a change in s_c no greater than ±0.01% (absolute). A more conservative uncertainty of s_c ±0.02% (absolute) is assigned for the reacted activation curves.

Supplementary results and discussion

Partitioning of nitric acid to calcite under dry conditions

The reactions performed at 0% RH produced a set of interesting results that suggest that under dry conditions the calcite particles became extensively coated by nitric acid that condensed on the partially reacted particles but that much of the HNO_3 was unable to actually react with the $CaCO_3$ core. Figure S3 displays two different ATFOMS nitrate measurements, in addition to the usual

NO_2^-/CaO^+ peak area ratio that has been used thus far (Fig. 4), for the 0% RH reactions. All three indicate that the nitrate signal at HNO_3 exposures > 25 ppb s was close to or larger than that measured from pure 200 nm $Ca(NO_3)_2$ particles. However, these particles never achieved critical supersaturations as small as pure calcium nitrate (Fig. S3d). The predicted critical supersaturation of 200 nm $Ca(NO_3)_2$ particles (κ_{app} = 0.51) is 0.058%, below the lower SS limit of the CCNc of ~0.08%. Therefore, completely converted calcite particles that were 100% $Ca(NO_3)_2$ would be completely CCN active when measured in the CCNc, precluding the measurement of an activation curve. This was not observed, even at the largest HNO_3 exposure of 162 ppb s at 0% RH the particles were ~40% CCN-active at SS = 0.089%. However, the ATOFMS nitrate peak areas were much larger than from pure $Ca(NO_3)_2$ particles. The condensation of relatively large amounts of nitric acid to the surface of the partially reacted particle is the best explanation for this, particularly if HNO_3 produces larger $^{46}(NO_2)^-$ signals than $Ca(NO_3)_2$ does per molecule. The short reaction times in the flow tube may have limited the ability of the nitric acid reactant to react further with the calcium carbonate core. Additionally, the dry conditions may have limited the reaction to the particle surface if it became saturated with undissociated carbonic acid, as discussed in the main paper.

Supplementary figures

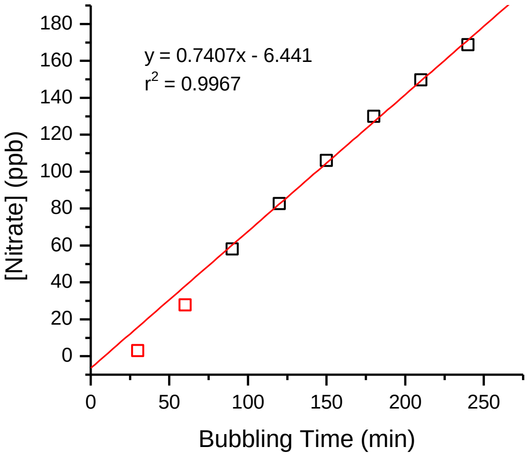

Figure S1. Calibration of HNO_3 permeation tube emission rate by bubbling gas stream into sodium carbonate buffer and measuring [NO_3^-] by ion chromatography in aliquots every 30 minutes. The first two aliquots (red symbol) are excluded from the linear fit.

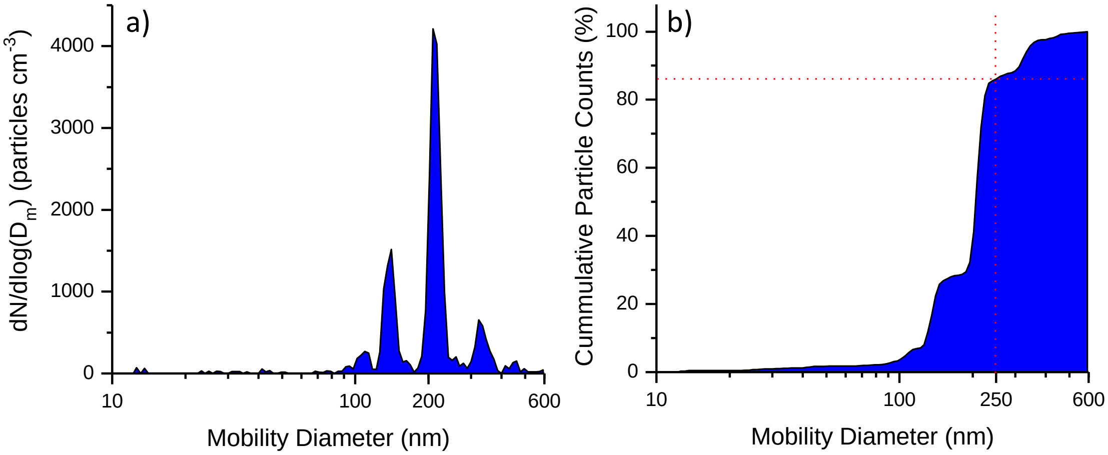

Figure S2. (a) Typical SMPS size distribution of size-selected calcite aerosol after reaction in the flow tube. (b) The % cumulative plot is used to determine the fraction of multiply charged particles of D_m > 250 nm. The SMPS charge correction was not used here.

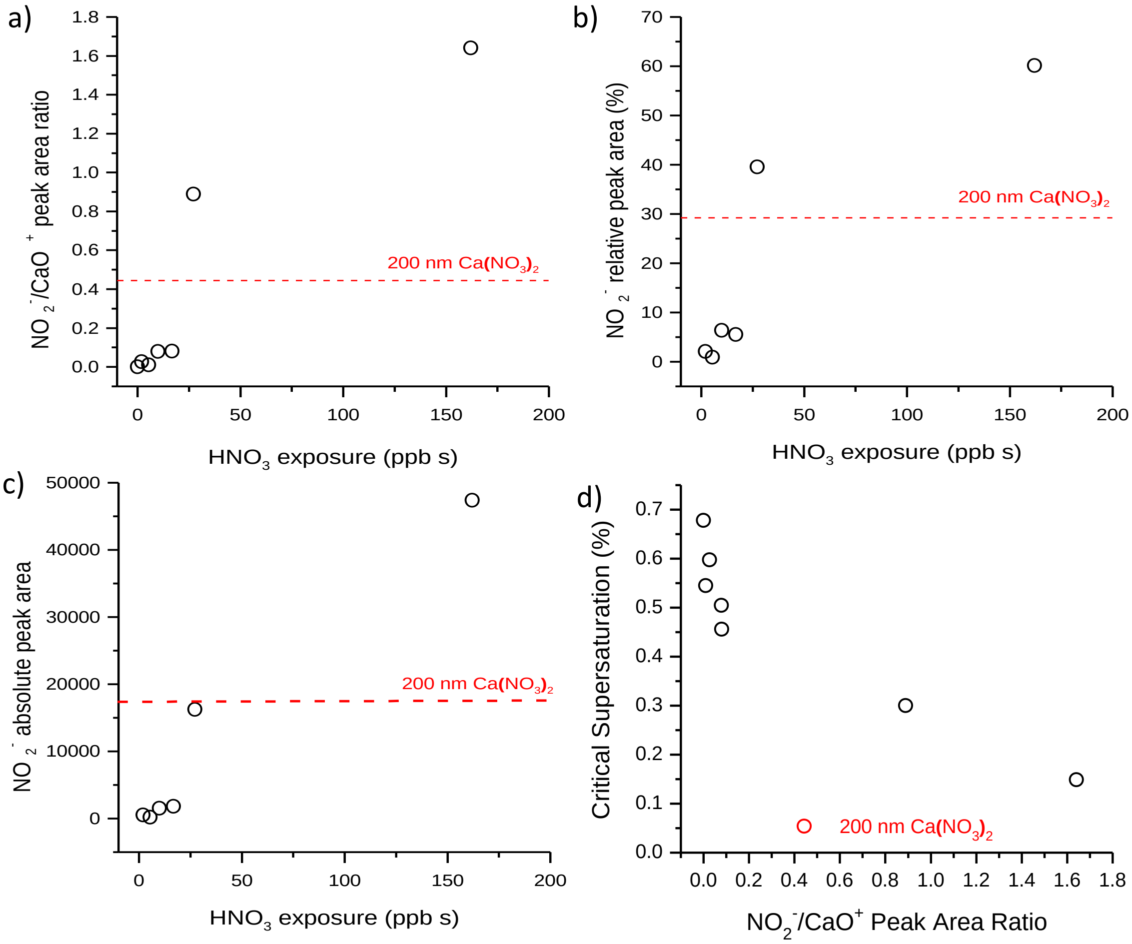

Figure S3. (a-c) Three ATOFMS nitrate metrics from calcite particles reacted with nitric acid at 0% relative humidity. Data from pure 200 nm calcium nitrate particles is included. (d) Critical supersaturation (s_c) of the same reacted particles versus the ATOFMS NO_2^-/CaO^+ absolute peak area ratio.